

Fig. 3. Dynamic ratio of sea-surface displacement to pressure as a function of phase velocity.

with the same phase velocity. That this is the case is shown in Fig. 3 where the ratio of ocean displacement to atmospheric pressure at sea level is plotted as a function of phase velocity. Resonant peaks are found in all the gravity modes, the ratio being at least ten times greater than the hydrostatic value for the phase-velocity range of 195 to 230 m/sec. Thus

amplitude build-up of the sea waves should begin before the arrival of the GW_0 group.

These results may be combined by Fourier synthesis to form a synthetic time series of sea-level displacement and atmospheric pressure as in Fig. 4. The first pressure pulse corresponds to the GR_0 mode and the accompanying sea wave is essentially the hydrostatic response. The main sea waves are in the GW_0 mode and propagate along great-circle paths with phase velocity near \sqrt{gH} . These are excited so efficiently by atmospheric waves with the same phase velocity that no corresponding large motion is shown on the pressure record. Intervening land barriers are jumped by the air waves which reexcite the sea wave if a sufficiently long fetch is available.

The theoretical group arrival times for the several modes and tsunami are shown in the tide-gage records of Fig. 1. It is seen that the sea waves begin and then reach large amplitudes in the interval between the GR_0 and GW_0 arrival times, as expected from the theory. The theoretical tsunami arrival times are too late, and the paths are

improbable for San Francisco, Honolulu, and Colon. South Georgia may have received direct tsunami waves. Colon shows large amplitudes beginning just after GR_0 and continuing through GW_0 . Its position near the antipodes, where the GR_0 waves are especially reinforced, may account for this. In view of the uncertain response of the instruments and the possibility of harbor resonances, no attempt was made to account for the absolute height or the spectrum of the sea waves.

Harkrider (3) showed how the properties of the source can be recovered from the pressure record. Using his scaling method, and data from nuclear explosions, we estimate that a surface explosion amounting to about 100 to 150 megatons would produce pressure pulses equivalent to those observed from Krakatoa.

FRANK PRESS

Department of Geology and
Geophysics, Massachusetts Institute
of Technology, Cambridge

DAVID HARKRIDER

Department of Geological Sciences,
Brown University, Providence,
Rhode Island

References and Notes

1. G. J. Symons, Ed., *The Eruption of Krakatoa and Subsequent Phenomena* (Trubner, London, 1888).
2. M. Ewing and F. Press, *Trans. Amer. Geophys. Union* **36**, 53 (1955).
3. F. Press and D. Harkrider, *J. Geophys. Res.* **67**, 3889 (1962); D. Harkrider, *ibid.* **69**, 5295 (1964).
4. Supported by ARPA and monitored by AFO contracts AF 49(638)-1632 and AF 49(638)-1693.

26 August 1966

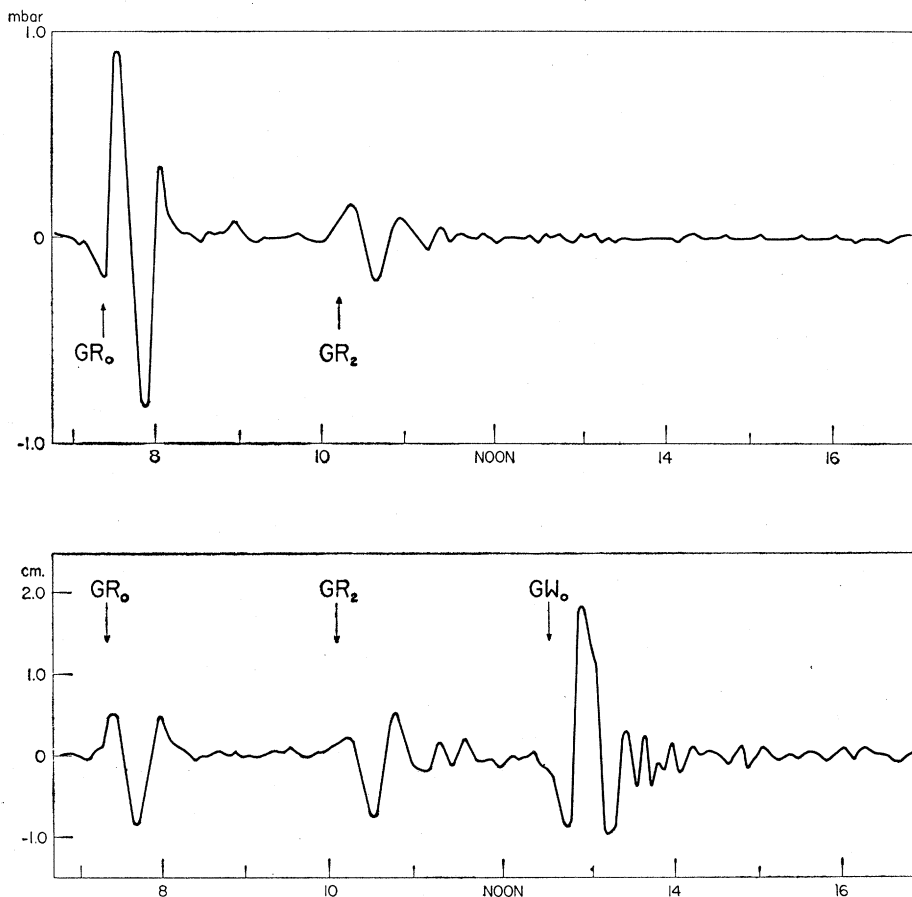


Fig. 4. Synthetic barogram (top) and marigram (bottom) for San Francisco. Source time function is a single-cycle sine wave of a 40-minute period. Time is local civil time, 27 August 1883.

Reversible Inactivation of Aged Solutions of Indolyl-3-Acetic Acid

Abstract. *Aqueous solutions of indole-3-acetic acid are inactivated by standing for a variable period of time. Inactivation results from conversion by oxidation of the plant hormone to polymerized deuteriauxin, which is depolymerized by boiling of the solution, which restores activity.*

Aqueous solutions of indole-3-acetic acid (IAA)—one of the most important plant hormones (auxins)—at physiological concentrations, say $5 \mu M$, are completely inactivated, as tested by the coleoptile cylinder bioassay (1), after a variable length of time. In our laboratory, complete inactivation may occur after a period of 24 to 48 hours. Figure 1 illustrates the results of two

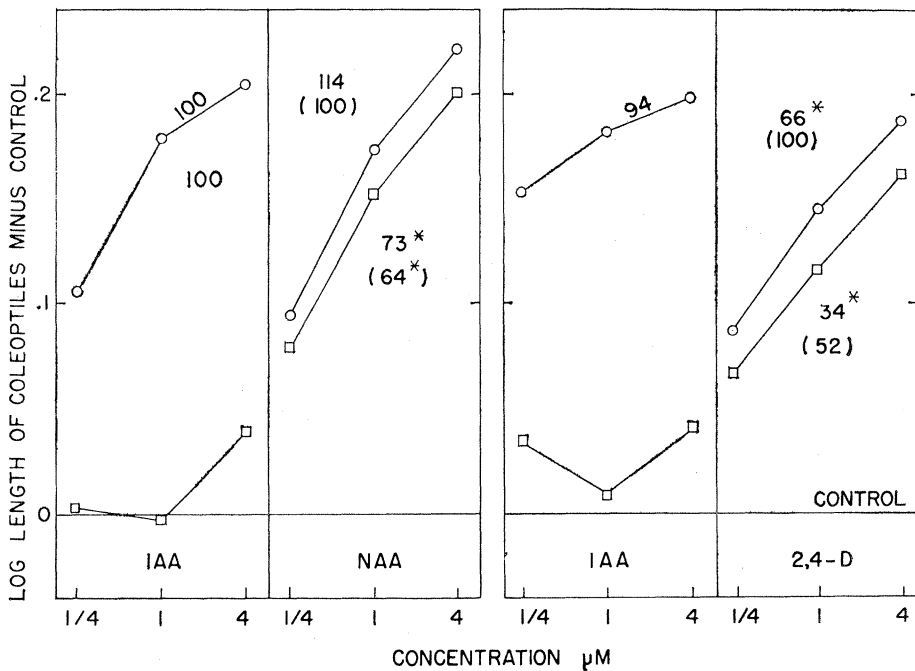
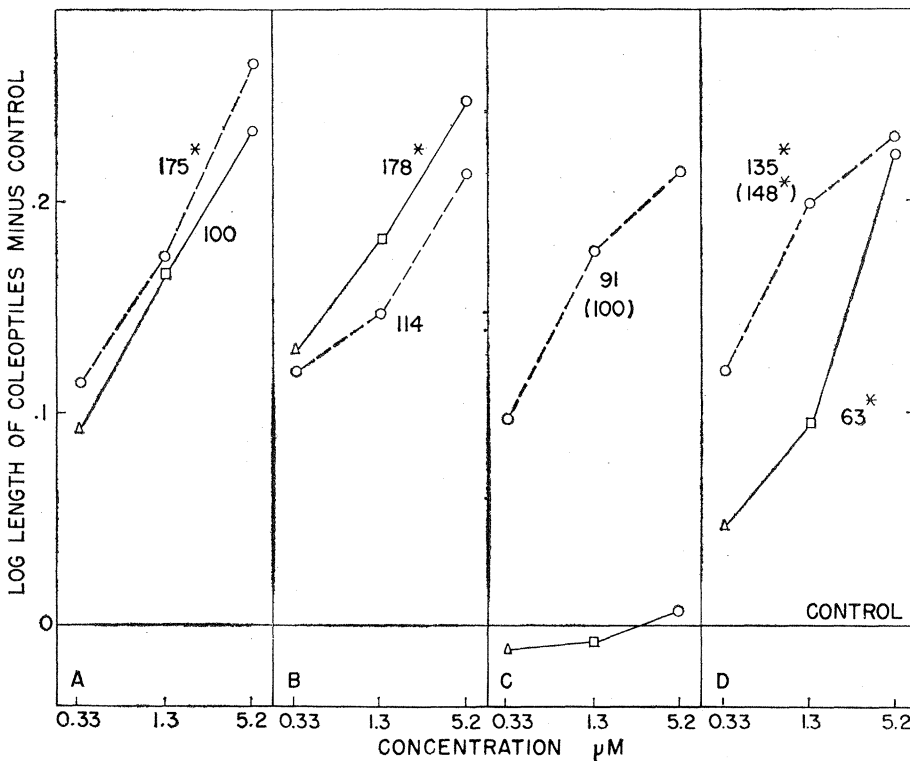


Fig. 1. Bioassay of fresh (○) and 24-hour (□) $4 \mu\text{M}$ aqueous solutions of IAA, α -naphthylacetic acid (NAA), and 2,4-dichlorophenoxyacetic acid (2,4-D) in 2 percent sucrose, buffered at pH 5. All solutions and their 1/4 and 1/16 dilutions were tested as 0.3 ml of the solution in small cups containing two 3-mm *Avena* coleoptile cylinders; there were ten replicates. The lengths of the cylinders after 18 hours in the solutions were measured with a logarithmic scale on blown-up ($\times 5$) shadowgraphs. Each point is the mean of 20 measurements, expressed in logarithms, of the length of coleoptiles, from which was deducted the mean for the control solution (coleoptiles in the test solution without auxin). The potency of each solution was compared with that of the fresh solution of IAA, to which was given an arbitrary value of 100. Only the means at the higher and lower concentrations were used in computation [four-point bioassay (7)]. Relative potencies, statistically significant at the 95 percent fiducial level, are indicated by an asterisk. Potencies between parentheses refer to the aged/fresh ratio of the solutions of NAA and of 2,4-D. The ratio of potency of the fresh IAA solutions prepared at a 2-day interval was not statistically significant as indicated by the four-point bioassay of the parallel portions (at the two higher concentrations) of their activity curves.



independent tests, made at a 2-day interval, in January (summer in the Southern Hemisphere), of the activities of fresh solutions and of 24-hour aged solutions of IAA in comparison with the activities of equimolar solutions of α -naphthylacetic acid and 2,4-dichlorophenoxyacetic acid. Whereas after 24 hours the IAA solutions were completely inactivated, the activity of α -naphthylacetic acid was reduced to 64 percent and that of 2,4-dichlorophenoxyacetic acid to 52 percent. The same experiments, performed at different times of the year, showed that, in the conditions of our laboratory, complete inactivation of IAA usually occurs within 24 hours in summer and in the fall, but may take 48 hours or more in winter and in the spring.

Inactivation of IAA results from auto-oxidation and does not occur when the solution is protected by an appropriate antioxidant such as cobaltous chloride (Fig. 2). No protection was afforded by reductants such as sodium thiosulfate or ascorbic acid at the concentrations used. Oxidants such as the vapor of iodine or of nitric acid, as well as ultraviolet radiation and the surface effect of porcelain chips in the solution, greatly hasten inactivation.

For short periods of aging, inactivation is reversible and activity is restored by simple boiling of the solution for 1 minute. In the experiment shown in Fig. 2, activity was restored to the extent of 63 percent. Up to 100 percent and more was observed in some other experiments. After prolonged aging, however, inactivation is irreversible and activity is not even partially restored by boiling.

Auto-oxidation of IAA can best be followed spectrophotometrically through the changes in the ultraviolet spectrum of solutions at a concentra-

Fig. 2 (left). Effect of aging (24 hours), of boiling, and of cobaltous chloride (broken lines), at the concentration of $5.2\text{-}\mu\text{M}$ solutions of IAA. Bioassay as in Fig. 1, each point representing the mean of ten measurements, and each test solution, buffered at pH 5, containing cobaltous chloride at the indicated concentrations (○, $10 \mu\text{M}$; □, $2.5 \mu\text{M}$; △, $0.63 \mu\text{M}$). (A, B) Fresh solutions and their 1/4 and 1/16 dilutions before (A) and after (B) boiling; (C, D) 24-hour solutions, under the same conditions. The relative potency of the cobalt containing 24-hour solutions, before and after boiling, is indicated in parentheses.

tion of 20 mg/liter for the triple-peaked band between 270 and 290 $m\mu$ or 5 mg/liter for the peak at 219 $m\mu$. The same changes are observed in eluates of IAA spotted on filter paper, standing for a variable length of time in the diffuse light of the laboratory (2). The great lability of IAA under those conditions has been used for an investigation of smog which showed that auto-oxidation of IAA is delayed in an air-conditioned laboratory as compared with one not air-conditioned. Hourly, daily, and seasonal variations have been observed (3).

Oxidation of solutions of IAA converts it to deuteriauxin, which in turn polymerizes and gathers on the surface as a very thin film (4). This film, examined under the microscope, is seen to be made up of coalesced, slightly refringent disks, about 10 μ in diameter. The disks produced on the surfaces of dilute solutions are not visible under the optical microscope but can be collected on copper grids and observed in the electron microscope. They exhibit circular electron diffraction bands corresponding to spacings of reticular planes of 1.2, 2.0, and 3.7 \AA (5).

Conversion of IAA to deuteriauxin, which polymerizes and thus becomes unavailable to the coleoptile sections, explains the early, reversible stages of inactivation. The film disappears by boiling, and restoration of activity by heat may be due to simple depolymerization of deuteriauxin.

Inactivation also occurs in nonbuffered solutions, although it is less pro-

nounced than in acidic solutions. It may, at least in part, account for the so-called "occasional" variations observed in the coleoptile elongation test which has usually a duration of 24 hours (1).

Hull *et al.* (6) have attributed to air pollutants the daily and seasonal fluctuations in sensitivity of the *Avena* curvature test. These authors suggest that decreased sensitivity is an effect on the growth response of the coleoptile and does not lie in the destruction of applied IAA by the pollutants. In the light of the present work, it seems likely that decreased sensitivity is an indirect effect of inactivation of endogenous auxin by air pollutants.

It would seem that reversible inactivation of IAA through the in vivo effect of oxidizing agents may play an important role in plant growth regulation.

A. A. BITANCOURT

*Plant Cancer Research Center,
Instituto Biológico,
São Paulo, Brazil*

References and Notes

1. J. A. Bentley, *J. Exptl. Botany* **1**, 201 (1950).
2. A. A. Bitancourt and G. M. De Fazio, *Ciência Cult. (São Paulo)* **18**, 236 (1966).
3. G. M. De Fazio and A. A. Bitancourt, *ibid.*, p. 237.
4. A. A. Bitancourt, *Nature* **200**, 548 (1963).
5. I am indebted to A. Bruner, Instituto Butantan, São Paulo, for the electron micrographs, and to the staff of Professor Trillat's laboratory, Centre National de la Recherche Scientifique, Bellevue, France, for the electron diffraction photographs cited in the text.
6. H. M. Hull, F. W. Went, N. Yamada, *Plant Physiol.* **29**, 182 (1954).
7. C. I. Bliss, *J. Am. Statist. Assoc.* **39**, 479 (1944).
8. Aided by a grant from the Technical Programs Division, USDA.

23 September 1966

Surface Recrystallization of Polyethylene Extended-Chain Crystals

Abstract. *Rough fracture surfaces of extended-chain polyethylene crystals become unstable at temperatures below the bulk melting point. There is no way for the extended chains, which are up to 20,000 methylene units long, to change position without collapse. As a result, the rough surfaces smooth out on heating by covering themselves with oriented folded-chain lamellae.*

Flexible, linear high-polymer molecules like polyethylene are difficult to transform from the random melt to an equilibrium crystal in which all chains are parallel and fully extended. The long chains, typically 10 to 100,000 \AA , cannot be added to a growing crystal in one step. The crystallization path leads first to thin folded-chain crystal lamellae which subsequently tend to re-arrange to a thermodynamically more

stable crystal with extended chains. The folded-chain lamellae are often only of the order of 100 \AA thick. On their path to the fully extended-chain crystal they normally freeze into a metastable state with only little larger fold length (1). Recently, using high-pressure techniques (2), we have grown almost fully extended-chain crystals of polyethylene. The character of the resulting material is completely changed.

Instead of a tough plastic, a brittle polycrystalline aggregate results. A fracture surface of such extended-chain material which was crystallized at 4350 atm and 227°C for 20 hours followed by 1.6°C per hour cooling is shown in an electron micrograph (Fig. 1). Of interest is the rough appearance of the fracture surface of the crystals. The many striations are at right angles to the lamellar surface, parallel to direction of the molecular chain (3). We carried out a statistical analysis of the surface roughness and were able to show that a similar surface structure would be formed by a crack propagating through a crystal, the crack taking randomly a left or right path around any molecular chain it encounters (4). Many surface chains are thus in elevated ridges with a large specific surface area and have been rendered less stable than the bulk by the process of fracturing.

We now report on the study of a property of the rough fracture surface. The extended-chain bulk polyethylene melts at 138.7°C (5). The surface stability was investigated by heating the identical fracture surface of Fig. 1 for 3 minutes to 120°C. On replication we searched for the same location (Fig. 2). All lamellae are covered with "ripples" aligned normal to the original striations. The smaller striations have disappeared, and the bigger ones are more rounded.

The most likely explanation we can offer at this point is that the molecular chains in large surface area ridges become unstable at these temperatures and tend to reorganize in order to reduce surface area. Since there is no way to roll stretched flexible polymer chains from a ridge into a valley, they collapse first by complete or partial melting. As a result, the chains have then the same restriction any polymer melt has in crystallization. Folded-chain crystals must be grown first even if an extended-chain crystal is present as a nucleus (6). These folded chain crystals are seen in Fig. 2 directly as ripples. The alignment of the crystallographic chain with the substrate is preserved so that in many cases the orientation of the substrate chain can be deduced from the ripple direction.

The observation of surface recrystallization of extended-chain crystals must be compared to three other observations. (i) Drawing folded-chain single crystals, Geil found that fibers are pulled out when cracks form which are not parallel to growth faces. When